

Resolving the Hubble tension in a $U(1)_{L_\mu-L_\tau}$ model with Majoron

Takeshi Araki¹, Kento Asai², Kei Honda³, Ryuta Kasuya³, Joe Sato³, Takashi Shimomura⁴,
Masaki J.S. Yang³

¹*Faculty of Dentistry, Ohu University, 31-1 Sankakudo, Tomita-machi, Koriyama, Fukushima 963-8611, Japan*

²*Department of Physics, University of Tokyo, Bunkyo-ku, Tokyo 113-0033, Japan*

³*Department of Physics, Saitama University, 255 Shimo-Okubo, Sakura-ku, Saitama 338-8570, Japan*

⁴*Faculty of Education, University of Miyazaki, 1-1 Gakuen-Kibanadai-Nishi, Miyazaki 889-2192, Japan*

Abstract

In this paper, we explore possibilities of resolving the Hubble tension and $(g-2)_\mu$ anomaly simultaneously in a $U(1)_{L_\mu-L_\tau}$ model with Majoron. We only focus on a case where the Majoron ϕ does not exist at the beginning of the universe and is created by neutrino inverse decay $\nu\nu \rightarrow \phi$ after electron-positron annihilation. In this case, contributions of the new gauge boson Z' and Majoron ϕ to the effective number of neutrino species N_{eff} can be calculated in separate periods. These contribution are labelled N'_{eff} for the $U(1)_{L_\mu-L_\tau}$ gauge boson and $\Delta N'_{\text{eff}}$ for the Majoron. The effective number $N_{\text{eff}} = N'_{\text{eff}} + \Delta N'_{\text{eff}}$ is evaluated by the evolution equations of the temperatures and the chemical potentials of light particles in each period.

As a result, we found that the heavier Z' mass $m_{Z'}$ results in the smaller N'_{eff} and requires the larger $\Delta N'_{\text{eff}}$ to resolve the Hubble tension. Therefore, compared to previous studies, the parameter region where the Hubble tension can be resolved is slightly shifted toward the larger value of $m_{Z'}$.

1 Introduction

Recently, a discrepancy has been reported on the values of the Hubble constant H_0 from the cosmic microwave background (CMB) measurements [1] and local measurements [2–5]. The inferred value from the Λ CDM with the temperature anisotropy of the CMB measured by Planck [1] is $H_0 = 67.36 \pm 0.54$ km/s/Mpc. On the other hand, the local measurements using Cepheids [2, 3] and type-Ia supernovae [4] by SH0ES reported larger values as $H_0 = 73.45 \pm 1.66$ km/s/Mpc and 74.03 ± 1.42 km/s/Mpc, respectively. A similar value of H_0 has been also reported by H0LiCOW from gravitational lensing with late time [5]. These local measurements result in a larger value of H_0 than the CMB measurement¹. The discrepancy reaches the level of $4 - 6\sigma$ and is called the Hubble tension.

Although the tension could originate from systematic errors in the measurements [8–10], it would indicate modifications of the standard cosmological model. Then, several solutions have been proposed in the fields of cosmology and particle physics. One of the approaches to solve the tension is to modify the effective number of neutrino species N_{eff} . In Ref. [1], combining the results from the CMB, Cepheids and others, N_{eff} is derived as 3.27 ± 0.15 at 68% C.L. [11], which implies the difference from the Λ CDM results as $0.2 \lesssim \Delta N_{\text{eff}} \lesssim 0.5$ to ameliorate the Hubble tension.² Such a difference can be obtained when new interactions with neutrinos exist. In this regard, models with gauged $U(1)_{L_\mu-L_\tau}$ symmetry are very interesting [14–17], under which only mu and tau-type leptons are charged. It is well-known that the long-standing discrepancy of the muon anomalous magnetic moment, $(g-2)_\mu$, can be resolved by the contributions of the new gauge boson Z' with an MeV scale mass [18–20]. The new interaction also alters the decoupling time of neutrinos from the thermal bath at the early universe. In particular, the decays of Z' to heat neutrinos lead to the increase of N_{eff} . In Ref. [21], it was shown that the Hubble tension can be solved simultaneously with the discrepancy of $(g-2)_\mu$.

Other interesting models are the ones with global Lepton number symmetry $U(1)_L$. In the class of seesaw mechanism, tiny neutrino masses are explained by the heavy Majorana masses of right-handed neutrinos which often can be generated by the spontaneous breaking of the Lepton number symmetry. As a result, a pseudo Nambu-Goldstone boson, the so-called Majoron, appears in the spectrum [22–25]. In Ref. [26], the decay of the Majoron with a keV scale mass can increase ΔN_{eff} at most 0.11 and hence help to ameliorate the Hubble tension.

Some models with $U(1)_{L_\mu-L_\tau}$ symmetry can reproduce observed neutrino masses and mixing by introducing global $U(1)_L$ symmetry [27]. In such models, the contributions from both the Z' boson and Majoron have to be taken into account by tracking the number and energy densities of light particles in the early universe. In this paper, we consider solutions of the Hubble tension in a $U(1)_{L_\mu-L_\tau}$ model with a Majoron by including contributions of all light particles. For simplicity, we only focus on a case where the Majoron does not exist at the beginning of the universe and is created by $\nu\nu \rightarrow \phi$ after e^\pm annihilation. In this case, N_{eff} can be calculated separately from the contribution of Z' boson and that of ϕ .

This paper is organized as follows. In section 2, we describe the $U(1)_{L_\mu-L_\tau}$ model with the global $U(1)_L$ symmetry. In section 3, we derive the evolution equations of the temperature and chemical potential in the early universe. In section 4, we solve these equations in order to

¹Local measurements based on the TRGB method [6] and TDCOSMO+SLACS analyses [7] reported consistent values to the CMB results.

²We should note that increasing N_{eff} worsens another milder tension relative to σ_8 [12, 13] that is the cosmological parameter about the matter density fluctuation amplitude on 8 Mpc scales.

calculate the contribution of Z' and Majoron to N_{eff} and impose a constraint on Z' and Majoron parameter space. Finally, we summarize our results in section 5.

2 $U(1)_{L_\mu-L_\tau}$ Model

We consider a $U(1)_{L_\mu-L_\tau}$ model which contains the global $U(1)_L$ symmetry, similarly to Ref. [27]. Such a model can have a keV Majoron as a pseudo Nambu-Goldstone boson (pNG boson) originated from the spontaneous symmetry breaking of the $U(1)_L$. In addition, this model has a $U(1)_{L_\mu-L_\tau}$ gauge boson, which can explain the muon anomalous magnetic moment and the IceCube gap of cosmic neutrino flux if this gauge boson has $\mathcal{O}(10-100)$ MeV mass [28–31]. As discussed in Refs. [21, 26], these particles can contribute to the expansion history of the early universe and have a possibility to resolve the Hubble tension.

In this section, we show the interactions between the electron, neutrino, $U(1)_{L_\mu-L_\tau}$ gauge boson Z' , and Majoron ϕ , which contribute to the Hubble parameter in the early universe.

2.1 The $U(1)_{L_\mu-L_\tau}$ Lagrangian

The Lagrangian related to the $U(1)_{L_\mu-L_\tau}$ gauge boson is given by

$$\mathcal{L}_{Z'} = -\frac{1}{4}Z'^{\rho\sigma}Z'_{\rho\sigma} + \frac{1}{2}m_{Z'}^2Z'^\rho Z'_\rho + g_{\mu-\tau}Z'_\rho J_{\mu-\tau}^\rho, \quad (1)$$

where Z' denotes the $U(1)_{L_\mu-L_\tau}$ gauge boson with the field strength $Z'_{\rho\sigma} = \partial_\rho Z'_\sigma - \partial_\sigma Z'_\rho$, and $m_{Z'}$ and $g_{\mu-\tau}$ are the $U(1)_{L_\mu-L_\tau}$ gauge boson mass and gauge coupling constant, respectively. $J_{\mu-\tau}$ denotes the $L_\mu - L_\tau$ current and is written by

$$J_{\mu-\tau}^\rho = \bar{\mu}\gamma^\rho\mu + \bar{\nu}_\mu\gamma^\rho P_L\nu_\mu - \bar{\tau}\gamma^\rho\tau - \bar{\nu}_\tau\gamma^\rho P_L\nu_\tau. \quad (2)$$

At tree level, the $U(1)_{L_\mu-L_\tau}$ gauge boson interacts only with mu and tau-type leptons.

2.2 Effective coupling with electrons

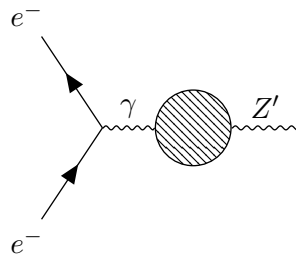


Figure 1: One-loop diagram which induces an interaction between Z' and electrons.

In this model, there can be a gauge kinetic mixing χ between Z' and the SM hypercharge gauge field B : $\mathcal{L}_{\text{mix}} = -\frac{\chi}{2}B^{\rho\sigma}Z'_{\rho\sigma}$ where $B_{\mu\nu}$ is the field strength of B . Although we assume that this kinetic mixing vanishes at some high scale for simplicity, non-zero kinetic mixing appears

at one-loop level at a low energy scale. This kinetic mixing then induces an interaction between Z' and electrons through the mixing ϵ of Z' with the SM photon γ as shown in Fig 1, and the interaction term is described as follows :

$$\mathcal{L}_{Z'} \supset -\epsilon e Z'_\mu \bar{e} \gamma^\mu e , \quad (3)$$

where ϵ is calculated by

$$\epsilon \simeq \frac{e g_{\mu-\tau}}{12\pi^2} \log \frac{m_\tau^2}{m_\mu^2} \simeq \frac{g_{\mu-\tau}}{70} , \quad (4)$$

where e and m_ℓ are the electromagnetic charge and the mass of charged lepton ℓ .

The partial decay widths of Z' are given as follows:

$$\Gamma_{Z' \rightarrow e^- e^+} = \frac{(\epsilon e)^2 m_{Z'}}{12\pi} \left(1 + \frac{2m_e^2}{m_{Z'}^2} \right) \sqrt{1 - \frac{4m_e^2}{m_{Z'}^2}} , \quad (5)$$

$$\Gamma_{Z' \rightarrow \nu_{\mu,\tau} \bar{\nu}_{\mu,\tau}} = \frac{g_{\mu-\tau}^2 m_{Z'}}{24\pi} . \quad (6)$$

Hereafter, we assume that neutrino masses are negligible and taken to be massless. Note that the BABAR experiment excludes the $U(1)_{L_\mu-L_\tau}$ gauge boson with $m_{Z'} > 2m_\mu$ as a solution of the muon anomalous magnetic moment, and thus we assumed $m_{Z'} < m_\mu$.

2.3 Majoron interactions

The spontaneous breaking of the global $U(1)_L$ symmetry gives rise to a Nambu-Goldstone boson, called the Majoron ϕ . If the global $U(1)_L$ symmetry is slightly broken, then the Majoron has a tiny mass :

$$\mathcal{L}_{\text{mass}} = -\frac{1}{2} m_\phi^2 \phi^2 . \quad (7)$$

The interaction between the Majoron and neutrinos is described by

$$\mathcal{L}_{\text{int}} = g_{\alpha\beta} \bar{\nu}_{L,\alpha} \nu_{L,\beta}^c \phi + h.c. , \quad (8)$$

where $g_{\alpha\beta} = g_{\beta\alpha}$ is coupling constants and $\nu_{L,\alpha}^c \equiv (\nu_{L,\alpha})^c = C \bar{\nu}_{L,\alpha}^T$ with the charge conjugation matrix C . As we will see later, this interaction can have a significant impact on the early universe.

Using the projection operator as $\nu_{L,\alpha} = P_L \nu_\alpha$, we can rewrite the Lagrangian as

$$\begin{aligned} \mathcal{L}_{\text{int}} &= g_{\alpha\beta} \bar{\nu}_\alpha P_R C \bar{\nu}_\beta^T \phi + g_{\alpha\beta}^* \nu_\alpha^T C P_L \nu_\beta \phi \\ &= \sum_\alpha g_{\alpha\alpha} \bar{\nu}_\alpha P_R C \bar{\nu}_\alpha^T \phi + 2 \sum_{\alpha < \beta} g_{\alpha\beta} \bar{\nu}_\alpha P_R C \bar{\nu}_\beta^T \phi + \sum_\alpha g_{\alpha\alpha}^* \nu_\alpha^T C P_L \nu_\alpha \phi + 2 \sum_{\alpha < \beta} g_{\alpha\beta}^* \nu_\alpha^T C P_L \nu_\beta \phi . \end{aligned} \quad (9)$$

In the first equality, we used $C(\gamma^5)^T = \gamma^5 C$. From the above interactions, we obtain the decay width for $\phi \rightarrow \nu_\alpha \nu_\beta$, $\phi \rightarrow \bar{\nu}_\alpha \bar{\nu}_\beta$ as

$$\Gamma_{\phi \rightarrow \nu_\alpha \nu_\beta} = \Gamma_{\phi \rightarrow \bar{\nu}_\alpha \bar{\nu}_\beta} = \frac{|g_{\alpha\beta}|^2 m_\phi}{4\pi S_{\alpha\beta}} . \quad (10)$$

Here, $S_{\alpha\beta}$ is a symmetry factor satisfying $S_{\alpha\beta} = 2(\alpha = \beta)$, $S_{\alpha\beta} = 1(\alpha \neq \beta)$.

3 Time evolution equation of temperature and chemical potential

Here we consider the thermodynamics of the early universe in the presence of new light particles, Z' and the Majoron ϕ . In our study, we assume the following conditions :

1. As for the parameters of Z' , we focus on the region of $g_{\mu-\tau} \sim 10^{-4}$ - 10^{-3} and $m_{Z'} \sim 10$ MeV to solve the $(g-2)_\mu$ anomaly.
2. As for the Majoron-neutrino couplings given in Eq. (8), we focus on the region of $|g_{\alpha\beta}| \lesssim 10^{-7}$ in order to evade the constraints from the Big Bang Nucleosynthesis (BBN) [26], KamLAND-Zen [32], and SN1987A [33, 34].
3. We assume that there is no primordial abundance of Majorons, and they are produced after e^\pm annihilation through the inverse decay process $\nu\nu \rightarrow \phi^3$; this assumption corresponds to looking at the parameter region satisfying Eq. (41). Boltzmann equations with simultaneous contributions from Z' and ϕ are technically difficult to solve. We leave it for future work.

Under condition 2, the scattering and the annihilation processes of Majorons can be neglected, and only the decay and inverse decay of the Majoron $\phi \leftrightarrow \nu_\alpha\nu_\beta, \bar{\nu}_\alpha\bar{\nu}_\beta$ are relevant to our study. Moreover, because of condition 1, Z' becomes non-relativistic before e^\pm annihilation and decays mainly into neutrinos. On the other hand, from condition 3, Majorons are produced after e^\pm annihilation. Therefore, thermodynamics of Z' and ϕ can be considered separately, before and after the temperature $T_\gamma \sim 10^{-2}$ MeV at which the electrons and positrons have already annihilated. In the following subsections, the evolution equations are derived for each period.

3.1 Evolution equation before e^\pm annihilation

We consider the evolution equations for the universe before e^\pm annihilation, at which photons, neutrinos, electrons, and Z' exist. Following the previous studies [21, 35, 36], we make the following approximations in the calculation.

1. All the particles follow the thermal equilibrium distribution function.
2. In the collision terms, we use the Maxwell-Boltzmann statistics.
3. Neglect the electron mass m_e in the collision terms for the weak interaction processes.
4. Neglect the chemical potentials μ_i for all the particles i .

³The initial condition $n_\phi = 0$ in the early universe where $U(1)_L$ symmetry is restored would be guaranteed as follows. Let S be an original field of the Majoron when the $U(1)_L$ symmetry is unbroken. Here we consider situations where S develops a vacuum expectation value (vev) after weak bosons decouple ($T \ll m_{Z,W}/3$). If the field S is sufficiently heavy and is not created by the decay of other fields, the number density of S in the early universe is negligible. For example, in Ref. [27], the field S_L has a mass of about TeV that is greater than masses of heavy neutrinos $M_N \sim O(100)$ GeV and acquires a vev $\sim O(10^{-7})$ GeV. Thus, the initial condition $n_\phi = 0$ is justified.

5. The temperatures T_i of a particle i in the same thermal bath are equal; $T_\gamma = T_{e^-}$ and $T_{\nu_\alpha} = T_{Z'} \equiv T_\nu$ for $\alpha = e, \mu, \tau$.

Using these approximations, we obtain the evolution equations for the temperatures of photon T_γ and neutrinos T_ν as follows [21]:

$$\frac{dT_\nu}{dt} = - \left(\frac{\partial \rho_\nu}{\partial T_\nu} + \frac{\partial \rho_{Z'}}{\partial T_\nu} \right)^{-1} \left[4H\rho_\nu + 3H(\rho_{Z'} + P_{Z'}) - \frac{\delta \rho_\nu}{\delta t} - \frac{\delta \rho_{Z'}}{\delta t} \right], \quad (11)$$

$$\frac{dT_\gamma}{dt} = - \left(\frac{\partial \rho_\gamma}{\partial T_\gamma} + \frac{\partial \rho_e}{\partial T_\gamma} \right)^{-1} \left[4H\rho_\gamma + 3H(\rho_e + P_e) + \frac{\delta \rho_\nu}{\delta t} + \frac{\delta \rho_{Z'}}{\delta t} \right], \quad (12)$$

with ρ_i and P_i being the energy density and pressure of particle i , respectively, and H the Hubble parameter. Here, the energy transfer rates in Eqs. (11) and (12) are given by

$$\frac{\delta \rho_{Z'}}{\delta t} = \frac{3m_{Z'}^3}{2\pi^2} \left[T_\gamma K_2 \left(\frac{m_{Z'}}{T_\gamma} \right) - T_\nu K_2 \left(\frac{m_{Z'}}{T_\nu} \right) \right] \Gamma_{Z' \rightarrow e^+ e^-}, \quad (13)$$

$$\frac{\delta \rho_\nu}{\delta t} = \frac{4G_F^2}{\pi^5} \left[(g_{eL}^2 + g_{eR}^2) + 2(g_{\mu L}^2 + g_{\mu R}^2) \right] F(T_\gamma, T_\nu) + \frac{2(g_{\mu-\tau} \epsilon \epsilon)^2}{\pi^5 m_{Z'}^4} F(T_\gamma, T_\nu), \quad (14)$$

where G_F is the Fermi coupling constant, K_2 is the modified Bessel function of the second kind, and $g_{eL} = 1/2 + s_W^2$, $g_{eR} = s_W^2$, $g_{\mu L} = -1/2 + s_W^2$, and $g_{\mu R} = s_W^2$ with the sine of Weinberg angle $s_W \equiv \sin \theta_W$. The function $F(T_1, T_2)$ is defined as

$$F(T_1, T_2) = 32(T_1^9 - T_2^9) + 56T_1^4 T_2^4 (T_1 - T_2). \quad (15)$$

3.2 Evolution equation after e^\pm annihilation

We derive the evolution equations for the universe after e^\pm annihilation, at which photons, neutrinos, and the Majoron exist. In analogy with the previous subsection, we make the following assumptions [36].

1. All the particles follow the thermal equilibrium distribution function.
2. In the collision terms, we use the Maxwell-Boltzmann statistics.
3. $T_{\nu_\alpha} \equiv T_\nu$ and $\mu_{\nu_\alpha} \equiv \mu_\nu$ ($\alpha = e, \mu, \tau$).

Using these approximations, we obtain the evolution equations for temperature and chemical

potential as follows ⁴ [36] :

$$\frac{dT_\nu}{dt} = \left(\frac{\partial n_\nu}{\partial \mu_\nu} \frac{\partial \rho_\nu}{\partial T_\nu} - \frac{\partial n_\nu}{\partial T_\nu} \frac{\partial \rho_\nu}{\partial \mu_\nu} \right)^{-1} \left[-3H \left((\rho_\nu + P_\nu) \frac{\partial n_\nu}{\partial \mu_\nu} - n_\nu \frac{\partial \rho_\nu}{\partial \mu_\nu} \right) + \frac{\partial n_\nu}{\partial \mu_\nu} \frac{\delta \rho_\nu}{\delta t} - \frac{\partial \rho_\nu}{\partial \mu_\nu} \frac{\delta n_\nu}{\delta t} \right], \quad (16)$$

$$\frac{d\mu_\nu}{dt} = - \left(\frac{\partial n_\nu}{\partial \mu_\nu} \frac{\partial \rho_\nu}{\partial T_\nu} - \frac{\partial n_\nu}{\partial T_\nu} \frac{\partial \rho_\nu}{\partial \mu_\nu} \right)^{-1} \left[-3H \left((\rho_\nu + P_\nu) \frac{\partial n_\nu}{\partial T_\nu} - n_\nu \frac{\partial \rho_\nu}{\partial T_\nu} \right) + \frac{\partial n_\nu}{\partial T_\nu} \frac{\delta \rho_\nu}{\delta t} - \frac{\partial \rho_\nu}{\partial T_\nu} \frac{\delta n_\nu}{\delta t} \right], \quad (17)$$

$$\frac{dT_\phi}{dt} = \left(\frac{\partial n_\phi}{\partial \mu_\phi} \frac{\partial \rho_\phi}{\partial T_\phi} - \frac{\partial n_\phi}{\partial T_\phi} \frac{\partial \rho_\phi}{\partial \mu_\phi} \right)^{-1} \left[-3H \left((\rho_\phi + P_\phi) \frac{\partial n_\phi}{\partial \mu_\phi} - n_\phi \frac{\partial \rho_\phi}{\partial \mu_\phi} \right) + \frac{\partial n_\phi}{\partial \mu_\phi} \frac{\delta \rho_\phi}{\delta t} - \frac{\partial \rho_\phi}{\partial \mu_\phi} \frac{\delta n_\phi}{\delta t} \right], \quad (18)$$

$$\frac{d\mu_\phi}{dt} = - \left(\frac{\partial n_\phi}{\partial \mu_\phi} \frac{\partial \rho_\phi}{\partial T_\phi} - \frac{\partial n_\phi}{\partial T_\phi} \frac{\partial \rho_\phi}{\partial \mu_\phi} \right)^{-1} \left[-3H \left((\rho_\phi + P_\phi) \frac{\partial n_\phi}{\partial T_\phi} - n_\phi \frac{\partial \rho_\phi}{\partial T_\phi} \right) + \frac{\partial n_\phi}{\partial T_\phi} \frac{\delta \rho_\phi}{\delta t} - \frac{\partial \rho_\phi}{\partial T_\phi} \frac{\delta n_\phi}{\delta t} \right], \quad (19)$$

$$\frac{dT_\gamma}{dt} = -HT_\gamma, \quad (20)$$

with n_i being the number density of particle i . The number and energy density transfer rate of neutrinos are given by

$$\frac{\delta n_\nu}{\delta t} = \sum_\alpha \left(\frac{\delta n_{\nu\alpha}}{\delta t} + \frac{\delta n_{\bar{\nu}\alpha}}{\delta t} \right), \quad (21)$$

$$\frac{\delta \rho_\nu}{\delta t} = \sum_\alpha \left(\frac{\delta \rho_{\nu\alpha}}{\delta t} + \frac{\delta \rho_{\bar{\nu}\alpha}}{\delta t} \right). \quad (22)$$

Since ϕ and ν are no longer strongly coupled to the photon in this period, their chemical potentials are no longer guaranteed to be zero. Thus, the above evolution equations for μ_ν and μ_ϕ are indispensable.

3.3 Calculation of the number and energy transfer rates

To solve the evolution equations for temperatures and chemical potentials, we need to calculate the number and the energy transfer rates. For processes $\phi \leftrightarrow \nu_\alpha \nu_\beta$ and $\phi \leftrightarrow \bar{\nu}_\alpha \bar{\nu}_\beta$, the number and the energy transfer rate of ϕ are described as follows [36]:

$$\left. \frac{\delta n_\phi}{\delta t} \right|_{\phi \leftrightarrow \nu_\alpha \nu_\beta} = \left. \frac{\delta n_\phi}{\delta t} \right|_{\phi \leftrightarrow \bar{\nu}_\alpha \bar{\nu}_\beta} = \frac{m_\phi^2 \Gamma_{\phi \rightarrow \nu_\alpha \nu_\beta}}{2\pi^2} \left[T_\nu e^{2\mu_\nu/T_\nu} K_1 \left(\frac{m_\phi}{T_\nu} \right) - T_\phi e^{\mu_\phi/T_\phi} K_1 \left(\frac{m_\phi}{T_\phi} \right) \right], \quad (23)$$

$$\left. \frac{\delta \rho_\phi}{\delta t} \right|_{\phi \leftrightarrow \nu_\alpha \nu_\beta} = \left. \frac{\delta \rho_\phi}{\delta t} \right|_{\phi \leftrightarrow \bar{\nu}_\alpha \bar{\nu}_\beta} = \frac{m_\phi^3 \Gamma_{\phi \rightarrow \nu_\alpha \nu_\beta}}{2\pi^2} \left[T_\nu e^{2\mu_\nu/T_\nu} K_2 \left(\frac{m_\phi}{T_\nu} \right) - T_\phi e^{\mu_\phi/T_\phi} K_2 \left(\frac{m_\phi}{T_\phi} \right) \right]. \quad (24)$$

Actually, in addition to the decay and inverse decay of ϕ , there also exist the scattering and the annihilation processes of Majoron. However, we neglect these processes because we assume

⁴A derivation of these equations can be found in Appendix A.

$|g_{\alpha\beta}| \lesssim 10^{-7}$ as mentioned at the beginning of this section. In this case, the number transfer rate for ϕ is given by

$$\begin{aligned} \frac{\delta n_\phi}{\delta t} &= \sum_{\alpha \leq \beta} \left(\frac{\delta n_\phi}{\delta t} \Big|_{\phi \leftrightarrow \nu_\alpha \nu_\beta} + \frac{\delta n_\phi}{\delta t} \Big|_{\phi \leftrightarrow \bar{\nu}_\alpha \bar{\nu}_\beta} \right) \\ &= \frac{m_\phi^2 \Gamma_\phi}{2\pi^2} \left[T_\nu e^{2\mu_\nu/T_\nu} K_1 \left(\frac{m_\phi}{T_\nu} \right) - T_\phi e^{\mu_\phi/T_\phi} K_1 \left(\frac{m_\phi}{T_\phi} \right) \right], \end{aligned} \quad (25)$$

where Γ_ϕ is the total decay width of ϕ given by

$$\Gamma_\phi \equiv \sum_{\alpha \leq \beta} (\Gamma_{\phi \rightarrow \nu_\alpha \nu_\beta} + \Gamma_{\phi \rightarrow \bar{\nu}_\alpha \bar{\nu}_\beta}) = \frac{m_\phi \lambda^2}{4\pi}, \quad (26)$$

where $\lambda^2 \equiv \text{tr}(g^\dagger g)$. In the same way, the energy transfer rate for ϕ is written as

$$\begin{aligned} \frac{\delta \rho_\phi}{\delta t} &= \sum_{\alpha \leq \beta} \left(\frac{\delta \rho_\phi}{\delta t} \Big|_{\phi \leftrightarrow \nu_\alpha \nu_\beta} + \frac{\delta \rho_\phi}{\delta t} \Big|_{\phi \leftrightarrow \bar{\nu}_\alpha \bar{\nu}_\beta} \right) \\ &= \frac{m_\phi^3 \Gamma_\phi}{2\pi^2} \left[T_\nu e^{2\mu_\nu/T_\nu} K_2 \left(\frac{m_\phi}{T_\nu} \right) - T_\phi e^{\mu_\phi/T_\phi} K_2 \left(\frac{m_\phi}{T_\phi} \right) \right]. \end{aligned} \quad (27)$$

The transfer rates for neutrinos, $\delta n_\nu/\delta t$ and $\delta \rho_\nu/\delta t$, can be obtained from the number and the energy conservation law. In the present case, the physics does not depend on a basis of neutrinos, because the neutrino masses are neglected. This is understood from the fact that Γ_ϕ depends on $g_{\alpha\beta}$ only in the form $\text{tr}(g^\dagger g)$. Thus, without loss of generality, we can assume that $g_{\alpha\beta}$ has only diagonal components, and the number conservation is expressed as

$$\frac{\delta n_{\nu_\alpha}}{\delta t} \Big|_{\phi \leftrightarrow \nu_\alpha \nu_\alpha} = -2 \frac{\delta n_\phi}{\delta t} \Big|_{\phi \leftrightarrow \nu_\alpha \nu_\alpha}, \quad (28)$$

which leads to

$$\frac{\delta n_\nu}{\delta t} = \sum_\alpha \left(\frac{\delta n_{\nu_\alpha}}{\delta t} \Big|_{\phi \leftrightarrow \nu_\alpha \nu_\alpha} + \frac{\delta n_{\bar{\nu}_\alpha}}{\delta t} \Big|_{\phi \leftrightarrow \bar{\nu}_\alpha \bar{\nu}_\alpha} \right) = -2 \frac{\delta n_\phi}{\delta t}. \quad (29)$$

On the other hand, the energy conservation leads to

$$\frac{\delta \rho_{\nu_\alpha}}{\delta t} \Big|_{\phi \leftrightarrow \nu_\alpha \nu_\alpha} = - \frac{\delta \rho_\phi}{\delta t} \Big|_{\phi \leftrightarrow \nu_\alpha \nu_\alpha}. \quad (30)$$

From Eq. (30), $\delta \rho_\nu/\delta t$ is found to be

$$\frac{\delta \rho_\nu}{\delta t} = \sum_\alpha \left(\frac{\delta \rho_{\nu_\alpha}}{\delta t} \Big|_{\phi \leftrightarrow \nu_\alpha \nu_\alpha} + \frac{\delta \rho_{\bar{\nu}_\alpha}}{\delta t} \Big|_{\phi \leftrightarrow \bar{\nu}_\alpha \bar{\nu}_\alpha} \right) = - \frac{\delta \rho_\phi}{\delta t}. \quad (31)$$

4 Numerical calculation

In this section, we discuss the initial conditions and the parameters for the evolution equations of temperatures and the chemical potentials derived in the previous section and show the numerical results. The codes for calculations are partially based on NUDEC_BSM [36].

4.1 Initial conditions and integration range

Before e^\pm annihilation

We solve the system of differential equations (11) and (12) starting from $T_\gamma = T_\nu = 20$ MeV at which all the particles are in thermal equilibrium, to $T_\gamma \sim 10^{-2}$ MeV where the e^\pm annihilation has taken place.

After e^\pm annihilation

Let us consider solving the system of differential equations (16)-(20) from the temperature where the Majoron hardly exists. To see when the Majoron can be produced in the early universe, we can consider $\langle \Gamma_{\nu\nu \rightarrow \phi} \rangle / H$, where $\langle \Gamma_{\nu\nu \rightarrow \phi} \rangle$ is the thermally averaged neutrino inverse decay rate, and H is the Hubble rate. The ratio $\langle \Gamma_{\nu\nu \rightarrow \phi} \rangle / H$ is written as [36]

$$\frac{\langle \Gamma_{\nu\nu \rightarrow \phi} \rangle}{H} = \frac{1}{81K_1(3)} \Gamma_{\text{eff}} \left(\frac{m_\phi}{T_\nu} \right)^4 K_1 \left(\frac{m_\phi}{T_\nu} \right), \quad (32)$$

$$\Gamma_{\text{eff}} \equiv \frac{\langle \Gamma_{\nu\nu \rightarrow \phi} \rangle}{H} \Big|_{T_\nu = m_\phi/3} \simeq \left(\frac{\lambda}{4 \times 10^{-12}} \right)^2 \left(\frac{\text{keV}}{m_\phi} \right). \quad (33)$$

This is illustrated in Figure 2 in [36]. Imposing $\langle \Gamma_{\nu\nu \rightarrow \phi} \rangle / H < 10^{-4}$, we obtain the condition for T_ν as follows :

$$\frac{T_\nu}{m_\phi} > \left(\frac{\Gamma_{\text{eff}}}{81K_1(3) \times 10^{-4}} \right)^{1/3} \simeq 10 \Gamma_{\text{eff}}^{1/3}. \quad (34)$$

Here, we use the approximation $K_1(x) \sim 1/x$ (for $x < 1$) because the situation with $T_\nu/m_\phi > 1$ is what we want to consider. If we set the range $\Gamma_{\text{eff}} \leq 10^3$, the initial value of T_ν should satisfy $T_\nu \gtrsim 100m_\phi$. Thus, we will take

$$T_\nu = 100 m_\phi, \quad (35)$$

as the initial condition for T_ν . As the initial condition for T_γ/T_ν , we use the numerical values after e^\pm annihilation ($T_\gamma \simeq 10^{-2}$ MeV) obtained by solving equations (11) and (12).

The remaining initial conditions are determined so that $\rho_\phi/\rho_\nu < 10^{-12}$ is satisfied. Since the Majoron is ultra-relativistic in $T_\nu = 100 m_\phi$, we can treat the Majoron as a massless particle, so ρ_ϕ/ρ_ν is written by

$$\frac{\rho_\phi}{\rho_\nu} = \frac{1}{6} \left(\frac{T_\phi}{T_\nu} \right)^4 \frac{\text{Li}_4(e^{\mu_\phi/T_\phi})}{-\text{Li}_4(-e^{\mu_\nu/T_\nu})} = \frac{4}{21} \left(\frac{T_\phi}{T_\nu} \right)^4 \left(1 + a \frac{\mu_\phi}{T_\phi} - \frac{6}{7} a \frac{\mu_\nu}{T_\nu} + \dots \right). \quad (36)$$

Here, $\text{Li}_s(z)$ is Polylogarithm and $a \equiv \zeta(3)/\zeta(4) \sim 1.2/1.08 \sim 1.1$. Therefore, to satisfy $\rho_\phi/\rho_\nu < 10^{-12}$, the parameters should be

$$\frac{T_\phi}{T_\nu} \lesssim 10^{-3}, \quad \left| \frac{\mu_\phi}{T_\phi} \right| < 1, \quad \left| \frac{\mu_\nu}{T_\nu} \right| < 1, \quad (37)$$

This means that the condition for μ_ϕ is

$$\left| \frac{\mu_\phi}{T_\nu} \right| = \left| \frac{\mu_\phi}{T_\phi} \right| \frac{T_\phi}{T_\nu} < \frac{T_\phi}{T_\nu} \lesssim 10^{-3}. \quad (38)$$

Furthermore, since the Majoron is a boson, μ_ϕ must satisfy

$$\frac{\mu_\phi}{T_\nu} < \frac{m_\phi}{T_\nu} = 10^{-2}, \quad (39)$$

from $\mu_\phi \leq m_\phi$. Here, the equality sign is removed because the Bose-Einstein condensation cannot occur due to the very small number density of Majoron.

As the initial conditions that satisfies Eqs. (37)-(39), in this paper we take them as

$$\frac{T_\phi}{T_\nu} = 10^{-3}, \quad \frac{\mu_\nu}{T_\nu} = -10^{-4}, \quad \frac{\mu_\phi}{T_\nu} = -10^{-5}, \quad (40)$$

according to [36]. The differential equations are solved until $\rho_\phi/\rho_\nu < 10^{-6}$, when the Majoron has completely decayed away.⁵

4.2 Parameters

As mentioned before, we consider the case where the Majoron does not exist in the very early universe and is created after e^\pm annihilation ($T_\gamma \lesssim 10^{-2}\text{MeV}$). To realize this situation, the parameters of the Majoron must satisfy the following conditions :

- The Majoron production is most active after e^\pm annihilation.
- Shortly after e^\pm have annihilated ($T_\gamma \simeq 10^{-2}\text{MeV}$), the Majoron production is not yet effective.

Since $\langle \Gamma_{\nu\nu\rightarrow\phi} \rangle / H$ is maximal when $T_\nu \simeq m_\phi/3$ [36], the above conditions are expressed as

$$m_\phi/3 < 10^{-2} \text{ MeV}, \quad \left. \frac{\langle \Gamma_{\nu\nu\rightarrow\phi} \rangle}{H} \right|_{T_\nu=10^{-2} \text{ MeV}} < 1. \quad (41)$$

4.3 Results

Here, we show the results of solving the evolution equations derived in the previous section. In this study, the deviation of N_{eff} from the standard value occurs two times, namely before and after the e^\pm annihilation. Thus, it is convenient to write N_{eff} as

$$N_{\text{eff}} = N'_{\text{eff}} + \Delta N'_{\text{eff}}. \quad (42)$$

Here, N'_{eff} describes the effective number of neutrino species determined at $T_\nu/T_\gamma = \text{const.}$ soon after e^\pm annihilation and is defined as

$$N'_{\text{eff}} = 3 \left(\frac{11}{4} \right)^{4/3} \left(\frac{T_\nu}{T_\gamma} \right)^4 \Big|_{T_\gamma \simeq 10^{-2} \text{ MeV}}. \quad (43)$$

On the other hand, $\Delta N'_{\text{eff}}$ represents the change in the effective number of neutrino species due to the Majoron production after e^\pm annihilation. As we will see later, N'_{eff} and $\Delta N'_{\text{eff}}$ are not completely independent, and $\Delta N'_{\text{eff}}$ slightly depends on N'_{eff} .

⁵For $\Gamma_{\text{eff}} < 0.1$, we solve the equations until $\rho_\phi/\rho_\nu < 10^{-7}$ because it takes a long time for the Majoron to decay.

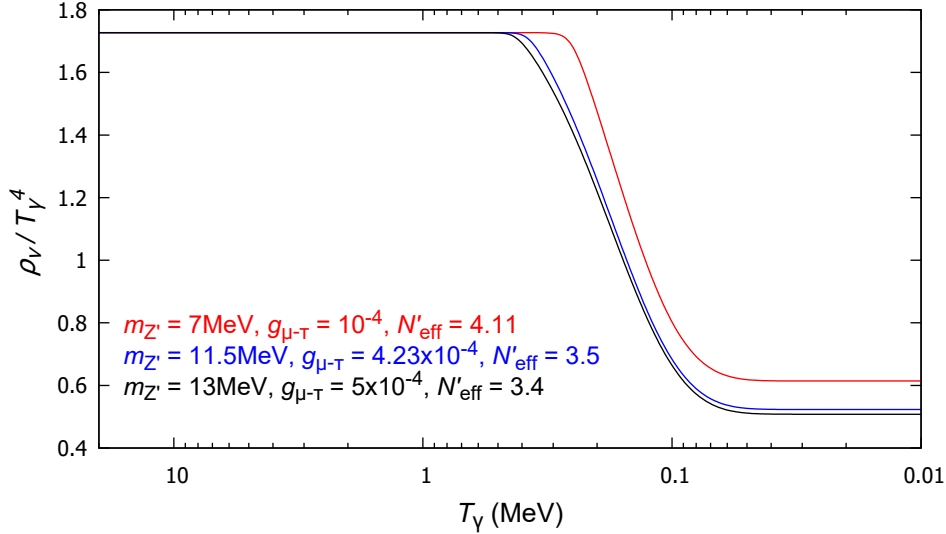


Figure 2: The evolution of the neutrino energy density for some Z' parameter.

Figure 2 shows the evolution of the neutrino temperature obtained by solving Eqs. (11) and (12). As can be seen from this figure, the value of N_{eff} is slightly larger than that of the SM $N_{\text{eff}}^{\text{SM}} \simeq 3.045$ [37, 38] due to the new gauge boson Z' .

Figure 3 shows the evolution of the neutrino energy density and the Majoron energy density for the case of $N'_{\text{eff}} = 3.5$. This figure shows that for $\Gamma_{\text{eff}} \gtrsim 1$, the Majoron begins to be produced by $\nu\nu \rightarrow \phi$ when the temperature reaches $T_\nu \gtrsim m_\phi$. After that, neutrinos and Majoron gradually reach the thermal equilibrium. This corresponds to the gently sloping area around the peak in the Figure 3. Since the net energy transfer due to $\phi \leftrightarrow \nu\nu$ is negligibly small, the evolution of the energy densities can be determined by the following Boltzmann equations:

$$\frac{d\rho_\nu}{dt} + 4H\rho_\nu = 0, \quad (44)$$

$$\frac{d\rho_\phi}{dt} + 3H(\rho_\phi + P_\phi) = 0. \quad (45)$$

At temperature $T_\nu \lesssim m_\phi$, the Majoron becomes non-relativistic and ρ_ϕ becomes much larger than P_ϕ . Consequently, the energy densities are derived as follows :

$$\rho_\nu \propto R^{-4}, \quad \rho_\phi \propto R^{-3}, \quad (46)$$

where R is the scale factor. Therefore, the difference between ρ_ν and ρ_ϕ occurs as the universe expands. At temperature $T_\nu \simeq m_\phi/3$, Majorons start to decay into neutrinos. Since the neutrinos produced by this decay are more energetic than the existing neutrinos, the overall neutrino energy density slightly increases, resulting in a slightly larger N_{eff} .

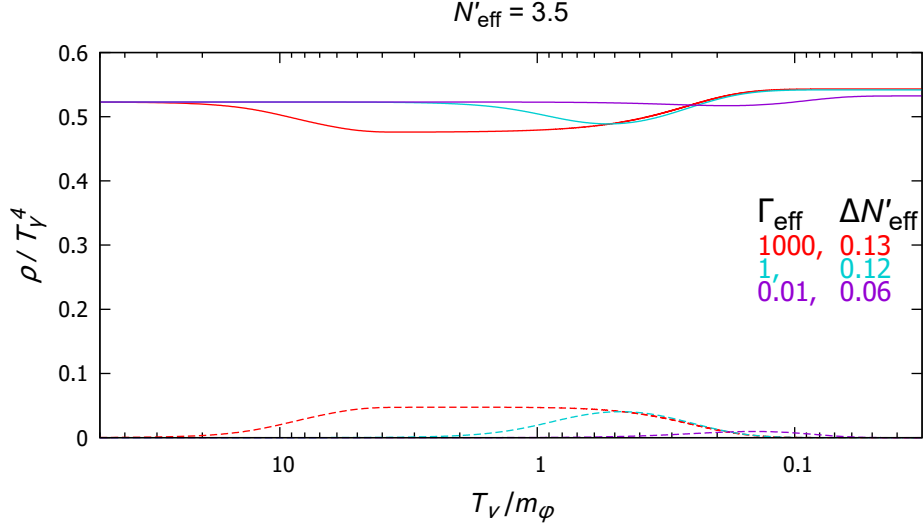


Figure 3: The evolution of neutrino (solid line) and Majoron (dashed line) energy density for the case of $N'_{\text{eff}} = 3.5$.

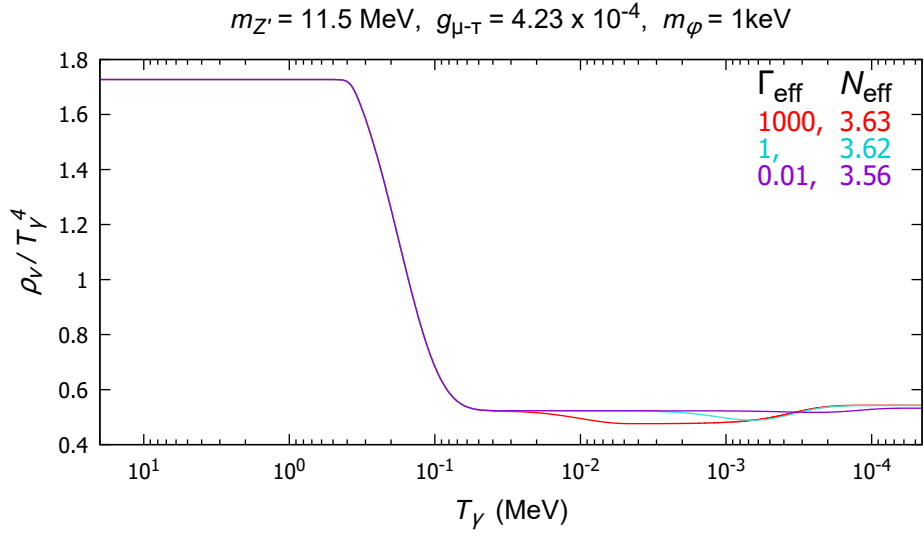


Figure 4: The evolution of the neutrino energy density for the case of $N'_{\text{eff}} = 3.5, m_\phi = 1 \text{ keV}$.

Figure 4 shows the evolution of the neutrino energy density for the case of $N'_{\text{eff}} = 3.5$, $m_\phi = 1$ keV. This figure is obtained by connecting Figure 2 and Figure 3 at $T_\gamma \simeq 10^{-2}$ MeV smoothly.

Figure 5 shows the Γ_{eff} dependence of $\Delta N'_{\text{eff}}$ for some N'_{eff} . The parameters $\Delta N'_{\text{eff}}$ and N'_{eff} are not completely independent, and $\Delta N'_{\text{eff}}$ slightly depends on N'_{eff} . As you can see, $\Delta N'_{\text{eff}}$ becomes larger for larger N'_{eff} . The reason is as follows : A large N'_{eff} corresponds to a large number of neutrinos after e^\pm annihilation. For $\Gamma_{\text{eff}} \gtrsim 1$, which corresponds to the case where the thermal equilibrium between the Majoron and neutrino is reached due to $\phi \leftrightarrow \nu\nu$, this process acts to equalize the number of neutrinos and Majorons. Thus, for the larger number of neutrinos after e^\pm annihilation, the more neutrinos are converted to the Majorons. As a result, the neutrino energy density at $T_\nu \ll m_\phi$ becomes larger, yielding an increase in $\Delta N'_{\text{eff}}$. On the other hand, for $\Gamma_{\text{eff}} \ll 1$, the thermal equilibrium is not achieved between ν and ϕ , but a small amount of Majoron is produced by $\nu\nu \rightarrow \phi$. This process occurs more often for a larger number of neutrinos after e^\pm annihilation. Thus, the production of Majoron increases slightly and it leads to an increase in $\Delta N'_{\text{eff}}$. Note that the contribution of Majoron $\Delta N'_{\text{eff}}$ cannot be larger than $\simeq 0.12$ in the case of the SM $N'_{\text{eff}} = 3.045$.

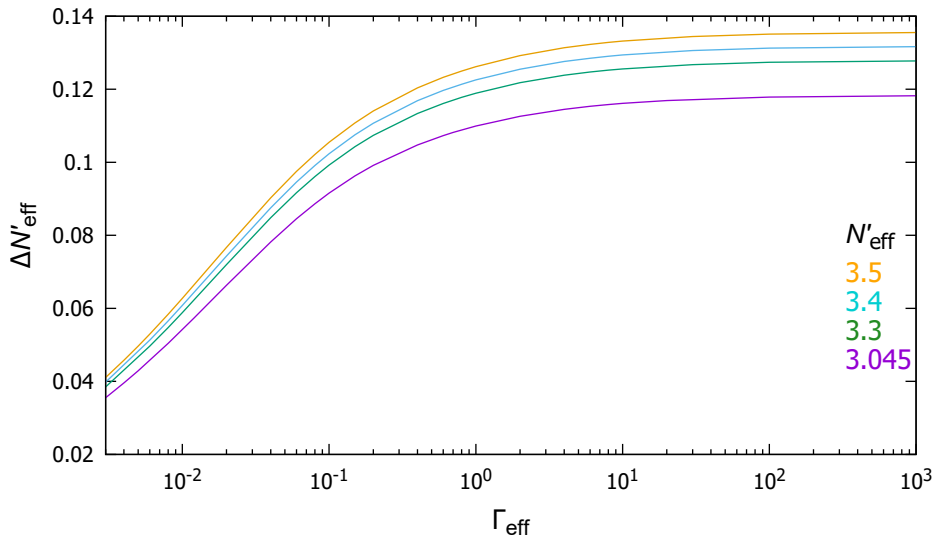


Figure 5: The Γ_{eff} dependence of $\Delta N'_{\text{eff}}$ for some N'_{eff} .

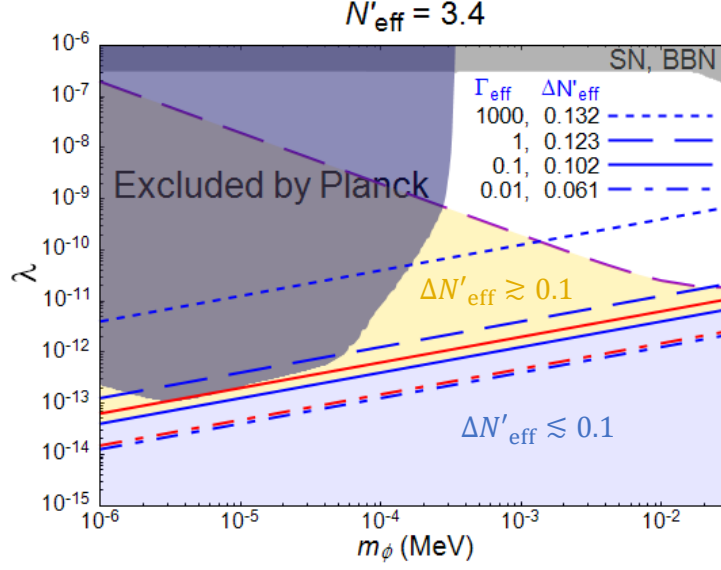


Figure 6: Parameter space of the Majoron in the presence of Z' that realizes $N'_{\text{eff}} = 3.4$. The solid and dotted blue lines are the contour lines of $\Delta N'_{\text{eff}}$ (Γ_{eff}). The solid and dotted red lines represent the same contour lines without Z' boson ($N'_{\text{eff}} = 3.045$). The area below the dashed purple line corresponds to one which satisfies Eq. (41). The gold region represents the region where $\Delta N'_{\text{eff}} \gtrsim 0.1$ holds. The blue region represents the parameter region where Hubble tensions can be resolved ($3.4 \lesssim N_{\text{eff}} \lesssim 3.5$). The dark blue region is excluded by Planck 2018 data [26]. The gray region is excluded by SN1987A [33, 34], Big Bang Nucleosynthesis (BBN) [26]. The white region cannot be treated in this paper.

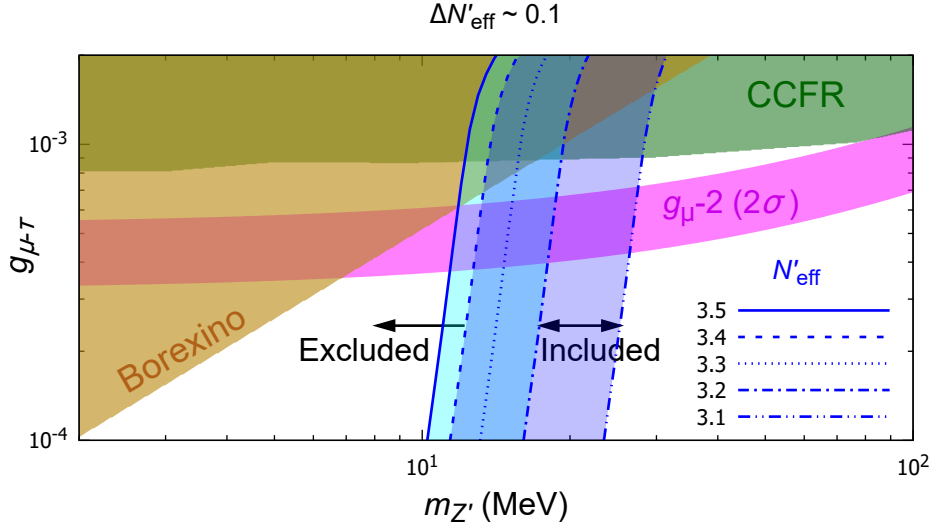


Figure 7: The Z' parameter space near the region where the $(g-2)_{\mu}$ anomaly can be resolved. The region between the solid and dashed dotted line ($3.2 \lesssim N'_{\text{eff}} \lesssim 3.5$) represents the region where the Hubble tension can be resolved only by Z' boson. The region between the dashed and dashed double-dotted line ($3.1 \lesssim N'_{\text{eff}} \lesssim 3.4$) represents the same region in the presence of Majoron that realizes $\Delta N'_{\text{eff}} \simeq 0.1$. The magenta band represents the region where the $(g-2)_{\mu}$ anomaly can be resolved within 2σ level [39]. The brown and green regions are excluded by the Borexino and CCFR experiments, respectively [40].

Using N'_{eff} and $\Delta N'_{\text{eff}}$ defined above, we can write N_{eff} as Eq. (42). If we fix either N'_{eff} or $\Delta N'_{\text{eff}}$, a constraint can be imposed on the other parameter by using the constraint from Planck 2018 : $N_{\text{eff}} = 3.27 \pm 0.15$ with 68% C.L.[11]. Although the various patterns are possible, we will only discuss the following two cases.

1. For $N'_{\text{eff}} \simeq 3.4$.

Figure 6 shows the parameter space of the Majoron in the presence of Z' that realizes $N'_{\text{eff}} = 3.4$. The solid and dotted blue lines are the contour lines of $\Delta N'_{\text{eff}}$ (Γ_{eff}). The solid and dotted red lines represent the same contour lines without Z' boson ($N'_{\text{eff}} = 3.045$). The area below the dashed purple line corresponds to Eq. (41). The blue region ($\Delta N'_{\text{eff}} \lesssim 0.1$) represents the region where the Hubble tension can be resolved ($3.4 \lesssim N_{\text{eff}} \lesssim 3.5$). The lower limit of the mass of the Majoron is taken to be 10^{-6} MeV because neutrino masses are not negligible below this value. The upper limit of Majoron mass (3×10^{-2} MeV) corresponds to the first condition in Eq. (41) $m_\phi/3 < 10^{-2}$ MeV. If Z' boson is in the parameter region where $(g-2)_\mu$ anomaly can be solved, the Hubble tension and the $(g-2)_\mu$ anomaly can be resolved simultaneously in the blue region. Furthermore, the gold region above the contour line of $\Delta N'_{\text{eff}} = 0.1$ is excluded at more than 2σ level.

2. For $\Delta N'_{\text{eff}} \simeq 0.1$.

Figure 7 shows the Z' parameter space near the region where the $(g-2)_\mu$ anomaly can be resolved. The region between the solid and dashed dotted line ($3.2 \lesssim N'_{\text{eff}} \lesssim 3.5$) represents the region where the Hubble tension can be resolved only by Z' boson, as in previous studies (*e.g.*, Fig. 5 in [21]). The region between the dashed and dashed double-dotted line ($3.1 \lesssim N'_{\text{eff}} \lesssim 3.4$) represents the same region in the presence of Majoron that realizes $\Delta N'_{\text{eff}} \simeq 0.1$. In this case, the parameter region where the Hubble tension can be resolved is slightly shifted toward the larger value of $m_{Z'}$. As a result, a new allowed region emerges for larger $m_{Z'}$. A choice of parameters $m_{Z'} \simeq 13 - 26$ MeV and $g_{\mu-\tau} \simeq (3.6 - 7) \times 10^{-4}$ can resolve the Hubble tension and $(g-2)_\mu$ anomaly simultaneously in the presence of Majoron. The region to the left of the $N'_{\text{eff}} = 3.4$ contour line is excluded at more than 2σ level.

5 Summary

In this paper, we explored possibilities of resolving the Hubble tension and $(g-2)_\mu$ anomaly simultaneously in realistic $U(1)_{L_\mu-L_\tau}$ models that can explain the origin of neutrino mass. In these models, there is a new light gauge boson Z' and a new light scalar, the Majoron ϕ . It arises from the spontaneous breaking of the global $U(1)_L$ symmetry and weakly couples to neutrinos. The parameters of Z' boson are set to be $10^{-3} \gtrsim g_{\mu-\tau} \gtrsim 10^{-4}$, $m_{Z'} \simeq 10$ MeV, neighborhoods of region that can resolve the $(g-2)_\mu$ anomaly.

We only focused on a case where the Majoron does not exist at the beginning of the universe and is created by $\nu\nu \rightarrow \phi$ after e^\pm annihilation. In this case, contributions of Z' and ϕ to the effective number N_{eff} can be calculated independently. Thus, it is convenient to write N_{eff} as $N_{\text{eff}} = N'_{\text{eff}} + \Delta N'_{\text{eff}}$, a sum of the effective number after e^\pm annihilations N'_{eff} and its change due to the Majoron $\Delta N'_{\text{eff}}$. The effective number N_{eff} is evaluated by evolution equations of temperatures and the chemical potentials of light particles in each period.

For simplicity, the following two cases are discussed. First, we explored the parameter space of the Majoron in the presence of Z' that realizes $N'_{\text{eff}} = 3.4$. In this case, the Hubble tension can be resolved ($N_{\text{eff}} \simeq 3.4 - 3.5$) in the wide region of the parameter space where $\Delta N'_{\text{eff}} \lesssim 0.1$ ($\lambda \lesssim 10^{-12} - 10^{-14}$) holds. On the other hand, the region with $\Delta N'_{\text{eff}} \gtrsim 0.1$ is excluded at more than 2σ level. In the second case, we surveyed the parameter region of Z' where the Hubble tension can be resolved in the presence of Majoron that realizes $\Delta N'_{\text{eff}} \simeq 0.1$. A choice of parameters $m_{Z'} \simeq 13 - 26 \text{ MeV}$, $g_{\mu-\tau} \simeq (3.6 - 7) \times 10^{-4}$ that corresponds to $N'_{\text{eff}} \simeq 3.1 - 3.4$ can resolve the Hubble tension and $(g - 2)_\mu$ anomaly simultaneously. On the other hand, the region with $m_{Z'} \lesssim 10 \text{ MeV}$ is excluded at more than 2σ level.

As a result, we found that the heavier $m_{Z'}$ results in the smaller N'_{eff} and requires the larger $\Delta N'_{\text{eff}}$ to resolve the Hubble tension. Therefore, compared to previous studies, the parameter region where the Hubble tension can be resolved is slightly shifted toward the larger value of $m_{Z'}$. Note that N'_{eff} and $\Delta N'_{\text{eff}}$ are not completely independent, and $\Delta N'_{\text{eff}}$ slightly depends on N'_{eff} .

Finally, Boltzmann equations with simultaneous contributions from Z' and ϕ are more difficult to solve. We leave it for future work.

Acknowledgments

This work was supported by JSPS KAKENHI Grants No. JP18H01210 (T.A., J.S., T.S., M.J.S.Y), No. JP19J13812 (K.A.), No. JP18K03651 (T.S.), No. 20K14459, (M.J.S.Y), and MEXT KAKENHI Grant No. JP18H05543 (J.S., T.S., M.J.S.Y).

A Derivation of the evolution equation after e^\pm annihilation

Here, we derive the evolution equations (16) to (19) after e^\pm annihilation. First of all, the evolution equations for the temperature T_a and chemical potential μ_a of a particle species a that follows the thermal equilibrium distribution function are given by [36]

$$\frac{dT_a}{dt} = \left(\frac{\partial n_a}{\partial \mu_a} \frac{\partial \rho_a}{\partial T_a} - \frac{\partial n_a}{\partial T_a} \frac{\partial \rho_a}{\partial \mu_a} \right)^{-1} \left[-3H \left((\rho_a + P_a) \frac{\partial n_a}{\partial \mu_a} - n_a \frac{\partial \rho_a}{\partial \mu_a} \right) + \frac{\partial n_a}{\partial \mu_a} \frac{\delta \rho_a}{\delta t} - \frac{\partial \rho_a}{\partial \mu_a} \frac{\delta n_a}{\delta t} \right], \quad (47)$$

$$\frac{d\mu_a}{dt} = - \left(\frac{\partial n_a}{\partial \mu_a} \frac{\partial \rho_a}{\partial T_a} - \frac{\partial n_a}{\partial T_a} \frac{\partial \rho_a}{\partial \mu_a} \right)^{-1} \left[-3H \left((\rho_a + P_a) \frac{\partial n_a}{\partial T_a} - n_a \frac{\partial \rho_a}{\partial T_a} \right) + \frac{\partial n_a}{\partial T_a} \frac{\delta \rho_a}{\delta t} - \frac{\partial \rho_a}{\partial T_a} \frac{\delta n_a}{\delta t} \right]. \quad (48)$$

In Eqs. (47) and (48), n_a , ρ_a , P_a are the particle number density, energy density, and pressure of a particle species a , respectively. From the approximations 3 in subsection 3.2 and $T_{\nu_\alpha} =$

$T_{\bar{\nu}_\alpha}$, $\mu_{\nu_\alpha} = \mu_{\bar{\nu}_\alpha}$, Eq. (47) for the neutrino and antineutrino leads to

$$\frac{dT_\nu}{dt} = \left(\frac{\partial n_{\nu_\alpha}}{\partial \mu_\nu} \frac{\partial \rho_{\nu_\alpha}}{\partial T_\nu} - \frac{\partial n_{\nu_\alpha}}{\partial T_\nu} \frac{\partial \rho_{\nu_\alpha}}{\partial \mu_\nu} \right)^{-1} \left[-3H \left((\rho_{\nu_\alpha} + P_{\nu_\alpha}) \frac{\partial n_{\nu_\alpha}}{\partial \mu_\nu} - n_{\nu_\alpha} \frac{\partial \rho_{\nu_\alpha}}{\partial \mu_\nu} \right) + \frac{\partial n_{\nu_\alpha}}{\partial \mu_\nu} \frac{\delta \rho_{\nu_\alpha}}{\delta t} - \frac{\partial \rho_{\nu_\alpha}}{\partial \mu_\nu} \frac{\delta n_{\nu_\alpha}}{\delta t} \right], \quad (49)$$

$$\frac{dT_\nu}{dt} = \left(\frac{\partial n_{\bar{\nu}_\alpha}}{\partial \mu_\nu} \frac{\partial \rho_{\bar{\nu}_\alpha}}{\partial T_\nu} - \frac{\partial n_{\bar{\nu}_\alpha}}{\partial T_\nu} \frac{\partial \rho_{\bar{\nu}_\alpha}}{\partial \mu_\nu} \right)^{-1} \left[-3H \left((\rho_{\bar{\nu}_\alpha} + P_{\bar{\nu}_\alpha}) \frac{\partial n_{\bar{\nu}_\alpha}}{\partial \mu_\nu} - n_{\bar{\nu}_\alpha} \frac{\partial \rho_{\bar{\nu}_\alpha}}{\partial \mu_\nu} \right) + \frac{\partial n_{\bar{\nu}_\alpha}}{\partial \mu_\nu} \frac{\delta \rho_{\bar{\nu}_\alpha}}{\delta t} - \frac{\partial \rho_{\bar{\nu}_\alpha}}{\partial \mu_\nu} \frac{\delta n_{\bar{\nu}_\alpha}}{\delta t} \right]. \quad (50)$$

In addition, each thermodynamic quantity for $\{\nu_\alpha\}$, $\{\bar{\nu}_\alpha\}$ is expressed by the particle number density n_ν , the energy density ρ_ν , and the pressure P_ν for the total neutrino :

$$n_{\nu_\alpha} = n_{\bar{\nu}_\alpha} = \frac{1}{6} n_\nu, \quad (51)$$

$$\rho_{\nu_\alpha} = \rho_{\bar{\nu}_\alpha} = \frac{1}{6} \rho_\nu, \quad (52)$$

$$P_{\nu_\alpha} = P_{\bar{\nu}_\alpha} = \frac{1}{6} P_\nu. \quad (53)$$

By adding both sides of Eqs. (49) and (50), and summing over all flavors, we obtain the evolution equation for T_ν (16). The evolution equation for μ_ν (17) can also be obtained in the same way.

For the Majoron evolution equation, by using eqs.(47) and (48) set to $a = \phi$, we obtain the evolution equations for T_ϕ (18) and μ_ϕ (19).

References

- [1] PLANCK collaboration, N. Aghanim et al., *Planck 2018 results. V. CMB power spectra and likelihoods*, *Astron. Astrophys.* **641** (2020) A5, [1907.12875].
- [2] A. G. Riess et al., *New Parallaxes of Galactic Cepheids from Spatially Scanning the Hubble Space Telescope: Implications for the Hubble Constant*, *Astrophys. J.* **855** (2018) 136, [1801.01120].
- [3] A. G. Riess et al., *Milky Way Cepheid Standards for Measuring Cosmic Distances and Application to Gaia DR2: Implications for the Hubble Constant*, *Astrophys. J.* **861** (2018) 126, [1804.10655].
- [4] A. G. Riess, S. Casertano, W. Yuan, L. M. Macri and D. Scolnic, *Large Magellanic Cloud Cepheid Standards Provide a 1% Foundation for the Determination of the Hubble Constant and Stronger Evidence for Physics beyond Λ CDM*, *Astrophys. J.* **876** (2019) 85, [1903.07603].
- [5] K. C. Wong et al., *HOLiCOW – XIII. A 2.4 per cent measurement of H_0 from lensed quasars: 5.3 σ tension between early- and late-Universe probes*, *Mon. Not. Roy. Astron. Soc.* **498** (2020) 1420–1439, [1907.04869].
- [6] W. L. Freedman et al., *The Carnegie-Chicago Hubble Program. VIII. An Independent Determination of the Hubble Constant Based on the Tip of the Red Giant Branch*, 1907.05922.
- [7] S. Birrer et al., *TDCOSMO - IV. Hierarchical time-delay cosmography – joint inference of the Hubble constant and galaxy density profiles*, *Astron. Astrophys.* **643** (2020) A165, [2007.02941].
- [8] G. Efstathiou, *H_0 Revisited*, *Mon. Not. Roy. Astron. Soc.* **440** (2014) 1138–1152, [1311.3461].
- [9] W. L. Freedman, *Cosmology at a Crossroads*, *Nature Astron.* **1** (2017) 0121, [1706.02739].
- [10] M. M. Ivanov, Y. Ali-Haïmoud and J. Lesgourgues, *H_0 tension or T_0 tension?*, *Phys. Rev. D* **102** (2020) 063515, [2005.10656].
- [11] PLANCK collaboration, N. Aghanim et al., *Planck 2018 results. VI. Cosmological parameters*, *Astron. Astrophys.* **641** (2020) A6, [1807.06209].
- [12] PLANCK collaboration, N. Aghanim et al., *Planck 2018 results. VI. Cosmological parameters*, *Astron. Astrophys.* **641** (2020) A6, [1807.06209].
- [13] H. Hildebrandt et al., *KiDS+VIKING-450: Cosmic shear tomography with optical and infrared data*, *Astron. Astrophys.* **633** (2020) A69, [1812.06076].
- [14] R. Foot, *New Physics From Electric Charge Quantization?*, *Mod. Phys. Lett.* **A6** (1991) 527–530.
- [15] X. He, G. C. Joshi, H. Lew and R. Volkas, *NEW Z-prime PHENOMENOLOGY*, *Phys. Rev. D* **43** (1991) 22–24.
- [16] R. Foot, X. G. He, H. Lew and R. R. Volkas, *Model for a light Z-prime boson*, *Phys. Rev.* **D50** (1994) 4571–4580, [hep-ph/9401250].
- [17] X.-G. He, G. C. Joshi, H. Lew and R. R. Volkas, *Simplest Z-prime model*, *Phys. Rev.* **D44** (1991) 2118–2132.
- [18] S. Gninenko and N. Krasnikov, *The Muon anomalous magnetic moment and a new light gauge boson*, *Phys. Lett. B* **513** (2001) 119, [hep-ph/0102222].
- [19] S. Baek, N. Deshpande, X. He and P. Ko, *Muon anomalous $g-2$ and gauged $L(\mu)$ - $L(\tau)$ models*, *Phys. Rev. D* **64** (2001) 055006, [hep-ph/0104141].

- [20] E. Ma, D. Roy and S. Roy, *Gauged $L(\mu) - L(\tau)$ with large muon anomalous magnetic moment and the bimaximal mixing of neutrinos*, *Phys. Lett. B* **525** (2002) 101–106, [[hep-ph/0110146](#)].
- [21] M. Escudero, D. Hooper, G. Krnjaic and M. Pierre, *Cosmology with A Very Light $L_\mu - L_\tau$ Gauge Boson*, *JHEP* **03** (2019) 071, [[1901.02010](#)].
- [22] Y. Chikashige, R. N. Mohapatra and R. D. Peccei, *Are There Real Goldstone Bosons Associated with Broken Lepton Number?*, *Phys. Lett. B* **98** (1981) 265–268.
- [23] G. B. Gelmini and M. Roncadelli, *Left-Handed Neutrino Mass Scale and Spontaneously Broken Lepton Number*, *Phys. Lett. B* **99** (1981) 411–415.
- [24] H. M. Georgi, S. L. Glashow and S. Nussinov, *Unconventional Model of Neutrino Masses*, *Nucl. Phys. B* **193** (1981) 297–316.
- [25] J. Schechter and J. W. F. Valle, *Neutrino Decay and Spontaneous Violation of Lepton Number*, *Phys. Rev. D* **25** (1982) 774.
- [26] M. Escudero and S. J. Witte, *A CMB search for the neutrino mass mechanism and its relation to the Hubble tension*, *Eur. Phys. J. C* **80** (2020) 294, [[1909.04044](#)].
- [27] T. Araki, K. Asai, J. Sato and T. Shimomura, *Low scale seesaw models for low scale $U(1)_{L_\mu - L_\tau}$ symmetry*, *Phys. Rev. D* **100** (2019) 095012, [[1909.08827](#)].
- [28] T. Araki, F. Kaneko, Y. Konishi, T. Ota, J. Sato and T. Shimomura, *Cosmic neutrino spectrum and the muon anomalous magnetic moment in the gauged $L_\mu - L_\tau$ model*, *Phys. Rev. D* **91** (2015) 037301, [[1409.4180](#)].
- [29] A. Kamada and H.-B. Yu, *Coherent Propagation of PeV Neutrinos and the Dip in the Neutrino Spectrum at IceCube*, *Phys. Rev. D* **92** (2015) 113004, [[1504.00711](#)].
- [30] T. Araki, F. Kaneko, T. Ota, J. Sato and T. Shimomura, *MeV scale leptonic force for cosmic neutrino spectrum and muon anomalous magnetic moment*, *Phys. Rev. D* **93** (2016) 013014, [[1508.07471](#)].
- [31] A. DiFranzo and D. Hooper, *Searching for MeV-Scale Gauge Bosons with IceCube*, *Phys. Rev. D* **92** (2015) 095007, [[1507.03015](#)].
- [32] KAMLAND-ZEN collaboration, A. Gando et al., *Limits on Majoron-emitting double-beta decays of Xe-136 in the KamLAND-Zen experiment*, *Phys. Rev. C* **86** (2012) 021601, [[1205.6372](#)].
- [33] M. Kachelriess, R. Tomas and J. W. F. Valle, *Supernova bounds on Majoron emitting decays of light neutrinos*, *Phys. Rev. D* **62** (2000) 023004, [[hep-ph/0001039](#)].
- [34] Y. Farzan, *Bounds on the coupling of the Majoron to light neutrinos from supernova cooling*, *Phys. Rev. D* **67** (2003) 073015, [[hep-ph/0211375](#)].
- [35] M. Escudero, *Neutrino decoupling beyond the Standard Model: CMB constraints on the Dark Matter mass with a fast and precise N_{eff} evaluation*, *JCAP* **02** (2019) 007, [[1812.05605](#)].
- [36] M. Escudero Abenza, *Precision early universe thermodynamics made simple: N_{eff} and neutrino decoupling in the Standard Model and beyond*, *JCAP* **05** (2020) 048, [[2001.04466](#)].
- [37] P. F. de Salas and S. Pastor, *Relic neutrino decoupling with flavour oscillations revisited*, *JCAP* **07** (2016) 051, [[1606.06986](#)].

- [38] K. Akita and M. Yamaguchi, *A precision calculation of relic neutrino decoupling*, *JCAP* **08** (2020) 012, [2005.07047].
- [39] MUON G-2 collaboration, B. Abi et al., *Measurement of the Positive Muon Anomalous Magnetic Moment to 0.46 ppm*, *Phys. Rev. Lett.* **126** (2021) 141801, [2104.03281].
- [40] T. Araki, S. Hoshino, T. Ota, J. Sato and T. Shimomura, *Detecting the $L_\mu - L_\tau$ gauge boson at Belle II*, *Phys. Rev. D* **95** (2017) 055006, [1702.01497].